

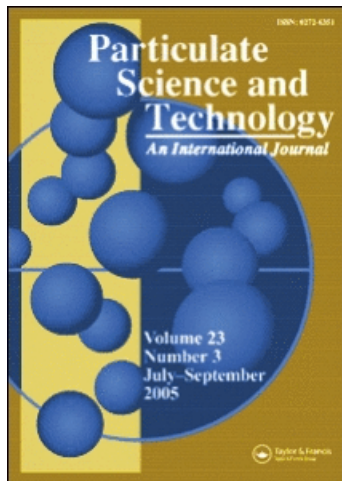
This article was downloaded by: [Kansas State University Libraries]

On: 18 September 2010

Access details: Access Details: [subscription number 917347143]

Publisher Taylor & Francis

Informa Ltd Registered in England and Wales Registered Number: 1072954 Registered office: Mortimer House, 37-41 Mortimer Street, London W1T 3JH, UK



Particulate Science and Technology

Publication details, including instructions for authors and subscription information:

<http://www.informaworld.com/smpp/title~content=t713774907>

Light Scattering as a Probe of Nanoparticle Aerosols

C. M. Sorensen^a

^a Department of Physics, Kansas State University, Manhattan, Kansas, USA

Online publication date: 15 September 2010

To cite this Article Sorensen, C. M.(2010) 'Light Scattering as a Probe of Nanoparticle Aerosols', Particulate Science and Technology, 28: 5, 442 – 457

To link to this Article: DOI: 10.1080/02726351.2010.504130

URL: <http://dx.doi.org/10.1080/02726351.2010.504130>

PLEASE SCROLL DOWN FOR ARTICLE

Full terms and conditions of use: <http://www.informaworld.com/terms-and-conditions-of-access.pdf>

This article may be used for research, teaching and private study purposes. Any substantial or systematic reproduction, re-distribution, re-selling, loan or sub-licensing, systematic supply or distribution in any form to anyone is expressly forbidden.

The publisher does not give any warranty express or implied or make any representation that the contents will be complete or accurate or up to date. The accuracy of any instructions, formulae and drug doses should be independently verified with primary sources. The publisher shall not be liable for any loss, actions, claims, proceedings, demand or costs or damages whatsoever or howsoever caused arising directly or indirectly in connection with or arising out of the use of this material.

Light Scattering as a Probe of Nanoparticle Aerosols

C. M. SORENSEN

Department of Physics, Kansas State University, Manhattan,
Kansas, USA

The purpose of this article is to review the potential for application of light scattering as a means to detect and measure nanoparticle aerosol systems. Key results are feasibility calculations for scattered intensity, anisotropy, and intensity correlation times relevant for both static and dynamic light scattering measurements. These calculations are set in the context of background scattering from the suspending gases and the growth of the particulate system via aggregation. Some specific examples are given, but general concepts are presented as recommendations to allow reader to plan their particular experiments.

Keywords aerosols, dynamic light scattering, light scattering, nanoparticles, particle sizing

Introduction

This article will explore light scattering's ability to sense and measure at the nanoscale. The first task is to determine whether enough light scatters to be detected above the necessary background scattering of the medium. The capabilities and limits of two types of static light scattering (SLS), structure factor and scattering/extinction measurement, and dynamic light scattering (DLS) will be considered. The conclusion will be that the nanoscale regime is very challenging for light scattering, but it is not entirely useless there.

Scattered Intensity

Rayleigh Scattering

One advantage of dealing with light scattering in the nanoscale range is that the small particle size (relative to λ) puts the problem in the Rayleigh scattering regime, which has a much simpler formulation than the general problem of Mie scattering for arbitrary size (Kerker 1969; Sorensen 2009). Typically the Rayleigh regime is defined as when

$$ka \ll 1 \quad (1)$$

The author's work on light scattering from aerosol systems has been supported by the NSF and NASA.

Address correspondence to C. M. Sorensen, Department of Physics, Cardwell Hall, Kansas State University, Manhattan, KS 66506-2601, USA. E-mail: sor@phys.ksu.edu

where $k = 2\pi/\lambda$, with λ the optical wavelength, and a is the radius of the particle. The product ka is often called the size parameter. Solving Equation (1) for the radius yields $a \ll \lambda/2\pi$. This article will take $\lambda = 500$ nm to allow for convenient numerical examples. This choice is reasonable since many sources such as argon ion ($\lambda = 488$ and 515 nm) and doubled YAG lasers ($\lambda = 532$ nm) are nearby (not as close is the HeNe laser at 633 nm). Then the Rayleigh condition requires a $\ll 80$ nm (diameter 160 nm).

Once within the Rayleigh approximation, which we have just seen is the case for nanoscale particles, particle shape ceases to be important. Simply put, the light cannot “see” shape when the particle is too small.

Consider light scattering where the incident and scattered directions define a horizontal scattering plane with a polarization perpendicular to this in the vertical direction. This is the common laboratory setup with a polarized laser as a source. Then, in the Rayleigh regime the differential cross section for scattering into the scattering plane is (Sorensen 2009)

$$\frac{dC_{\text{sca}}}{d\Omega} = k^4 a^6 \left| \frac{m^2 - 1}{m^2 + 2} \right|^2 \quad (2)$$

$$= k^4 a^6 F \quad (3)$$

where

$$F = \left| \frac{m^2 - 1}{m^2 + 2} \right|^2. \quad (4)$$

In Equations (2) and (4) m is the particle refractive index divided by the refractive index of the medium. The units of $dC_{\text{sca}}/d\Omega$ are $\text{cm}^2/\text{steradian}$ (hereafter steradian = sr). Note the a^6 functionality. This is one reason why light scattering from small particles is so difficult: they do not scatter much.

Scattering depends on both the scattering cross section per particle and the number of particles. To understand scattering, consider the drawing of an ensemble of particles in Figure 1. The scattering volume V_s is the visible, illuminated section of the sample. The width of the incident light beam defines the cross-sectional area A of the scattering volume. The length ℓ of the scattering volume is determined by the viewing optics. The probability of scattering the incident power P_o , which may be thought of as a number of photons per second, is proportional to the ratio of the total scattering cross-sectional area due to all the particles to the area of the beam. This is seen by the fact that the incident light sees the particles as effectively projected onto A , as drawn. We assume no overlap in the projections, a small scattering cross section approximation quite appropriate for nanoparticles. Thus, the probability for scattering per unit solid angle is

$$\text{prob} = N \frac{dC_{\text{sca}}}{d\Omega} A^{-1} \quad (5)$$

where N is the total number of particles in the scattering volume. The power scattered per unit solid angle is the scattered intensity I_s and is equal to the probability of scattering times the incident power:

$$I_s = N \frac{dC_{\text{sca}}}{d\Omega} A^{-1} P_o. \quad (6)$$

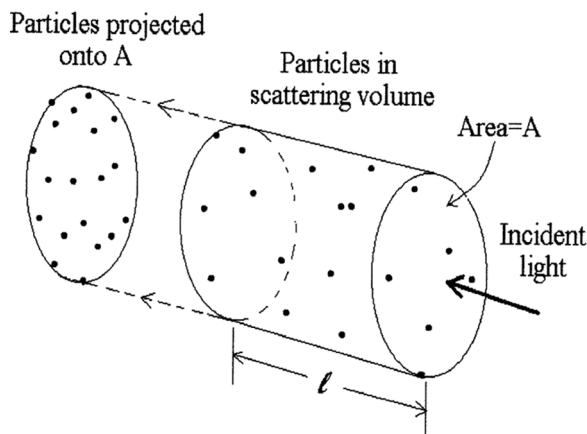


Figure 1. Diagram of how incident light sees particles in a scattering volume with volume $V_s = A\ell$ as projected onto the cross-sectional area A .

Now multiply and divide Equation (6) by the scattering volume length, ℓ , use $V_s = A\ell$ and the particle number density $n = N/V_s$ to yield

$$I_s = P_o \frac{dC_{sca}}{d\Omega} n\ell. \quad (7)$$

A very useful quantity resides in Equation (7), the Rayleigh ratio (Kerker 1969):

$$R_{vu} = n \frac{dC_{sca}}{d\Omega} \quad (8)$$

Combining Equations (7) and (8) yields

$$I_s = P_o R_{vu} \ell. \quad (9)$$

The first subscript v means the incident polarization is vertical, the second subscript u means unpolarized, i.e., no polarizer in front of the detector. The Rayleigh ratio is very useful because it describes the scattering from the whole system of particles by incorporating both the cross section for scattering per particle and the number density of particles. It is the probability of scattering per unit length of scattering volume. It is also useful because it allows for a direct comparison of the scattering strengths of particulate systems to those of some well-known gases and liquids.

Relative Scattering Strength

Table 1 gives Rayleigh ratios of some common substances. The Rayleigh ratio of air is $1.9 \times 10^{-8} \text{ cm}^{-1} \text{ sr}^{-1}$ at $\lambda = 500 \text{ nm}$. This is quite faint but certainly detectable in a darkened laboratory with incident laser powers of $\gtrsim 10 \text{ mW}$. Any particles suspended as an aerosol in air should have a R_{vu} comparable to air so that it can be detected above the background signal due to the air. Thus, in determining the feasibility of light scattering detection, it is reasonable to use $R_{uv} \simeq 10^{-8} \text{ cm}^{-1} \text{ sr}^{-1}$ as a lower limit for detectability. On the other hand, liquids have R_{vu} values approximately 10^3 times

Table 1. Rayleigh ratios ($10^{-6} \text{ cm}^{-1} \text{ sr}^{-1}$) at $T = 25^\circ\text{C}$, $p = 1 \text{ atm}$

Material	$\lambda = 514.5 \text{ nm}$	$\lambda = 488 \text{ nm}$
H ₂	0.0038	0.0047
Ar	0.0154	0.019
O ₂	0.0148	0.0183
N ₂	0.0173	0.0214
Air	0.0168	0.0208
CO ₂	0.034	0.042
CH ₄	0.0386	0.0477
Xe	0.0943	0.177
C ₂ H ₄	0.102	0.126
C ₂ H ₆	0.113	0.14

greater (similar to the density ratio). Scattering from simple liquids, e.g., toluene, CCl₄ (but not water, which is anomalous), is easily detectable, so a system R_{vu} value on the order of $10^{-5} \text{ cm}^{-1} \text{ sr}^{-1}$ can be considered quite feasible, especially for static light scattering measurements.

To consider nanoparticle scattering feasibility combine Equations (2) and (8) to find

$$R_{vu} = nk^4 a^6 \left| \frac{m^2 - 1}{m^2 + 2} \right|^2. \quad (10)$$

Let $\lambda = 500 \text{ nm}$ and $m = 1.5$, a typical value. Then n can be plotted as a function of a or, perhaps more in line with common usage, the particle diameter, $d = 2a$, for various values of R_{vu} . This is done in Figure 2, which can be viewed as a contour map in scattering strengths as parameterized by R_{vu} . As discussed above, a key contour is $R_{vu} = 10^{-8} \text{ cm}^{-1} \text{ sr}^{-1}$, because this represents about half the scattering strength of air, so any particulate aerosol with this R_{vu} value would be very difficult to detect and measure with light scattering because it is both faint and smaller than the scattering from the air background. (It is curious that if one assumes an “air molecule” has $d = 0.36 \text{ nm} = 3.6 \text{ \AA}$ and $m = 1.5$, and its number density at $T = 20^\circ$ and $p = 1 \text{ atm}$ is $n = 2.5 \times 10^{19} \text{ cm}^{-3}$, the ideal gas value, then $R_{vu} = 1.9 \times 10^{-8} \text{ cm}^{-1} \text{ sr}^{-1}$ the value for air.)

One obvious conclusion from Figure 2 is that if the particles are small all one needs is a high number density of them. This is usually acceptable for colloidal situations because then one can stabilize against aggregation. Not so for the aerosol systems, which are bound by kinetic theory to come together at a specified rate. High number density, necessary for an acceptable light scattering signal, brings fast aggregation times, which will limit any experiment.

Calculation of aggregation time scales in the nanoparticle regime is somewhat complex, potentially involving continuum, transition, and free molecular regimes (Seinfeld 1986; Oh and Sorensen 1997). However, for this light scattering feasibility study, an order of magnitude estimate of the time scales is sufficient. This can be achieved by using the continuum limit, which is algebraically straightforward. For room temperature ($T = 20^\circ\text{C}$) air this is inaccurate by no worse than a factor of four

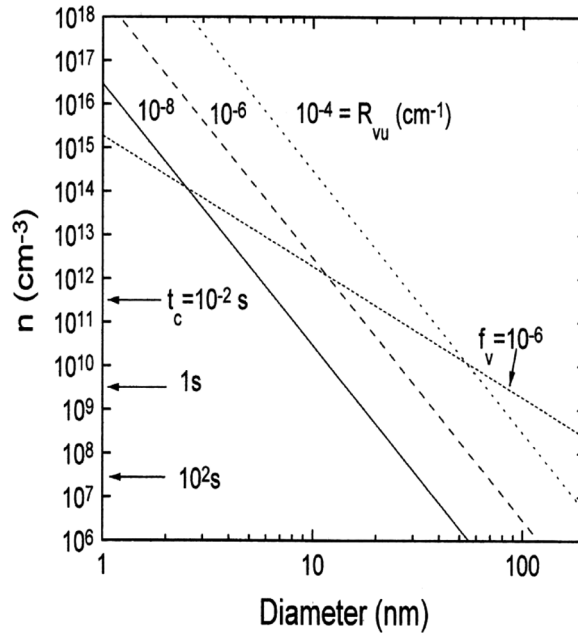


Figure 2. Number density n as a function of particle diameter for different Rayleigh ratio scattering values, R_{vu} , when $\lambda = 500$ nm and $m = 1.5$. Also shown are arrows indicating approximate concentrations for three aggregation times t_c for the particles in air at $T = 20^\circ\text{C}$ and $p = 1$ atm, and a line of constant volume fraction $f_v = 10^{-6}$.

as the particle size passes down from the continuum into the transition and free molecular regimes, so long as $a > 0.03$ nm. We define an aggregation time t_c as the time for the aerosol number density to decrease by a factor of two. One can show that (Oh and Sorensen 1997)

$$t_c = \left(\frac{4k_B T}{3\eta} n \right)^{-1} \quad (11)$$

where k_B is Boltzmann's constant, T the temperature, and η the gas viscosity. For room temperature air one finds

$$t_c = 3.3 \times 10^9 n^{-1} \quad (12)$$

with n in cm^{-3} . This value of t_c would decrease by almost a factor of two for air at 2000°C , which approximates a combustion environment. Three arrows indicating concentrations for three different t_c values are plotted in Figure 2.

A quick glance at Figure 2 shows that very large particle number concentrations are involved if we are to gain a detectable amount of scattered light. In general, that is the nature of nanoscale systems, lots of little pieces. An important quantity is the total amount of material per unit volume, which can be well described by the volume fraction, f_v ; for spherical particles $f_v = \pi d^3 n / 6$. Included in Figure 2 is a line for $f_v = 10^{-6}$, which can be used for reference. Note that in an aggregating system, mass is conserved so $f_v = \text{constant}$. Such a system would evolve with increasing d along a

line parallel to the $f_v = 10^{-6}$ line in Figure 2 to the right, and in doing so cross the lines of constant R_{vu} to larger values. This increased scattering as a conservative system coarsens is known as the Tyndall effect. One might say an inverse Tyndall effect plagues nanoscale systems, because if one subdivides at a constant volume fraction f_v , the system scatters less.

Figure 2 can help plan an experiment. For example, if one were to attempt a light scattering measurement on an aerosol of $d = 10$ nm particles, Figure 2 shows that a concentration of at least $n \simeq 3 \times 10^{10} \text{ cm}^{-3}$ is needed for the signal to be equal to that of the air medium. Figure 2 also shows that the aggregation time is $t_c \simeq 0.1$ s for this concentration, so the experiment needs to be done quickly. In fact, one should plan to continuously create the aerosol and flow it past the scattering volume. That way the age of the aerosol remains the same in the scattering volume. An example of this is a soot aerosol in a flame (Oh and Sorensen 1997; Gangopadhyay, Elminyaw, and Sorensen 1991; Sorensen, Cai, and Lu 1992; Kim et al. 2006). Initial monomer (primary) particle sizes are on the order $d = 10$ to 20 nm. Concentrations are typically $n \simeq 10^{12} \text{ cm}^{-3}$. Then Figure 2 shows $R_{vu} \simeq 10^4 \text{ cm}^{-1} \text{ sr}^{-1}$, quite bright, and indeed light scattering from soot in flames presents no trouble. Figure 2 or Equation (8), however, yields $t_c \simeq 10^{-3}$ s. Fortunately, flames flow quickly enough (~ 1 m/s) so that time is resolved into distance, and by keeping the scattering volume at one place in the flame, time must have a stop. The conclusion is that in flowing aerosols, if the number density can be made large enough, nanoparticle light scattering can be measured.

Static aerosols, e.g., an aerosol in a container, appear much more difficult. If one requires 10 s to make a measurement, then one should have $t_c \gtrsim 100$ sec. Thus, n must be less than $3 \times 10^7 \text{ cm}^{-3}$. At this value of n , $d \simeq 30$ nm would be on the edge of measurability. Not until $d \simeq 60$ nm would the scattered signal be readily detectable and even then rather dim. If instead a pulsed laser is used, measurement times can be drastically shortened. For example, many pulsed Nd:YAG lasers have ~ 10 ns pulses with repetition frequencies of tens of Hertz. Using the period of these pulses as the time scale, ~ 0.1 s, then, by Figure 2, $n \simeq 3 \times 10^{10} \text{ cm}^{-3}$ with $d \simeq 10$ nm is feasible. The time scale for one pulse is 10^{-8} s where, by Figure 2, concentrations of $n = 3 \times 10^{17} \text{ cm}^{-3}$ and $d < 1$ nm are possible.

Absolute Scattering Strength

Equation (9) can be used to calculate the absolute scattering for a typical experimental situation (whatever that is). Assume a continuous wave laser with $P_o = 1$ watt, which is quite strong. For $\lambda = 500$ nm, this is $P_o = 2.5 \times 10^{18}$ photons/s. Also, take $\ell = 0.3$ cm and let $R_{vu} = 10^{-8} \text{ cm}^{-1} \text{ sr}^{-1}$. To calculate the solid angle Ω assume a 2.5 mm diameter photocathode 25 cm away. This yields $\Omega = 7.8 \times 10^{-5}$ sr. This value could vary widely depending on experimental conditions. Our value is conservative and represents an angular spread of $\delta\theta \simeq 2.5 \text{ mm}/25 \text{ cm} \simeq 0.01$ radian $\simeq 0.6^\circ$. If instead the detector was very close, say only 2.5 cm away, then Ω would be two orders of magnitude larger, which is good for detection, but the angular spread would be larger as well at $\delta\theta = 6^\circ$, which is bad for defining the angle necessary for accurate size measurement. The scattered power at the detector is $P_s = I_s \Omega$. Then, using the conservative value of Ω , Equation (9) yields $I_s = 6 \times 10^5$ photons/s. Typical photomultiplier tubes have quantum efficiencies of ~ 10 to 20%; thus a photocount rate of $\sim 10^5$ counts/s would be observed. This is certainly large enough

to detect and measure. The implication is that for $R_{vu} = 10^{-8} \text{ cm}^{-1} \text{ sr}^{-1}$ and large laser power the scattering is strong enough to be well measured. Of course, as described above, it is only about half as strong as the scattering from the air medium.

It is hard to anticipate future experiments, so the following speculations probably will not cover all possibilities. Table 1 shows that the R_{vu} value for H_2 is $\sim 1/4$ of that for air. No doubt He has a low R_{vu} too. So these could be used as carrier gases for the nanoaerosol if it was desired to study it with light scattering. Also, R_{vu} is proportional to the absolute pressure so perhaps the gas background could be reduced at reduced pressure. Below, when we discuss dynamic light scattering, we will see that particle scattering has different dynamics than gas scattering. This will allow dynamic light scattering below the R_{vu} cutoff used here. Perhaps static measurements can also be filtered dynamically to remove the gas scattering background.

The ultimate limit is when P_s gets very small. Typical dark counts in PMTs are ~ 100 counts/s. This would occur when the aerosol $R_{vu} \simeq 10^{-11} \text{ cm}^{-1} \text{ sr}^{-1}$. Then, following the pattern in Figure 2, if $d = 10 \text{ nm}$, $n = 3 \times 10^7$ and $t_c = 100 \text{ s}$; comfortable values. If the larger solid angle of detection was used, $n = 3 \times 10^5$ could be detected for $d = 10 \text{ nm}$. This is a volume fraction of only 1.6×10^{-13} . PMTs can be cooled so that the dark count is ~ 1 count/s; new solid-state detectors have high quantum efficiency and low noise, etc. It is time to leave the desk and go to the lab with Figure 2 in mind to ultimately determine feasibility.

Static Light Scattering

Structure Factor Analysis

Structure factor analysis involves measuring the asymmetry of scattering as a function of angle (Sorensen 2001). In the near Rayleigh regime one finds the angular dependence of the differential cross section is well described by (Guinier et al. 1955; Sorensen and Shi 2000)

$$\frac{dC_{sca}}{d\Omega} = \left(\frac{dC_{sca}}{d\Omega} \right)_{\theta=0} \left(1 - \frac{1}{3} q^2 R_g^2 \right). \quad (13)$$

In Equation (13) R_g is the radius of gyration of the particle and q is the scattering wave vector given by

$$q = 4\pi\lambda^{-1} \sin(\theta/2), \quad (14)$$

where θ is the scattering angle. Even when significant asymmetry exists, the Rayleigh differential cross section, Equation (2), holds at zero scattering angle, as long as another parameter, the phase shift parameter, is small (Kerker 1969; Sorensen 2009). The phase shift parameter is defined by

$$\rho = 2ka|m - 1|, \quad (15)$$

The cross sections in Equation (13) are rather clumsy, but the equation is simply convertible to

$$I(q) = I(0) \left(1 - \frac{1}{3} q^2 R_g^2 \right), \quad (16)$$

where $I(q)$ is the scattered intensity at q . Equation (16) is the well-known Guinier equation (Guinier et al. 1955; Sorensen and Shi 2000) and is valid for all refractive indices and sizes, as long as $\rho < 1$ and $qR_g < 1$, and all shapes, including aggregates (Sorensen 2001). It applies when $qR_g < 1$, but often this restriction may be relaxed (Sorensen 2001). From an experimental point of view Equation (16) is more useful inverted as ($qR_g < 1$)

$$I(0)/I(q) = 1 + \frac{1}{3}q^2R_g^2. \quad (17)$$

Thus, by plotting inverse scattered intensity data versus q^2 a linear relation should result with slope equal to $R_g^2/3$.

Equations (16) and (17) can be applied to the problem of nanoparticle sizing. As before, take $\lambda = 500$ nm. Then, as θ ranges from 0 to 180° , q ranges from 0 to $2.5 \times 10^{-2} \text{ nm}^{-1}$. Inverse q is an important length scale; it is the resolution of the scattering (Oh and Sorensen 1999). Our maximum q is $2.5 \times 10^{-2} \text{ nm}^{-1}$ so our smallest (best) resolution is $q^{-1} = 40$ nm. This is an estimate of the smallest particles that can be measure with $\lambda = 500$ nm.

Equation (16) is plotted in Figure 3 for spheres where $d/2 = a = \sqrt{5/3}R_g$. This figure shows $d = 50$ nm particles cause at most only 8% anisotropy in the scattering. This is certainly measurable, but note that if the random error in the data was $\pm 2\%$, a pretty good value, d would be uncertain by $(2\%/8\%)$ $50 \text{ nm} = 12 \text{ nm}$, i.e., $d = 50 \pm 12 \text{ nm}$, not particularly good. Larger particles show greater anisotropy, and this is where the Guinier method is most useful. Examples of this usefulness abound in small angle X-ray scattering measurements, in light scattering measurements of macromolecules, where Equation (17) is the optical basis of the classical Zimm of biophysics plot, and in some of our work on aerosols (Kim et al. 2006). An example (Gangopadhyay, Elminyaw, and Sorensen 1991) of the latter is given

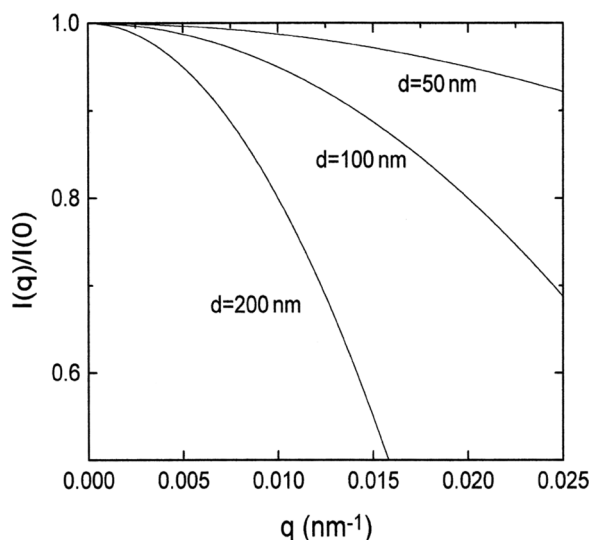


Figure 3. Plot of the Guinier scattering curve, Equation (16), for $\lambda = 500$ nm.

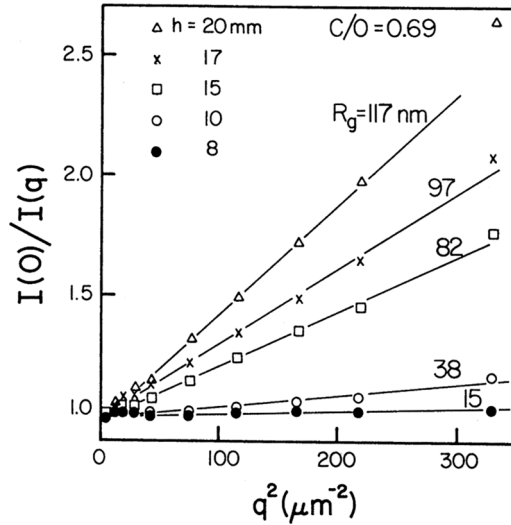


Figure 4. Flame soot data for premixed methane/oxygen plotted for a Guinier analysis, Equation (17). Flame parameters: C/O is the carbon-to-oxygen ratio, h is height above burner.

in Figure 4. In summary, it appears that optical structure factor measurements using the Guinier equation are limited to sizes of $d \gtrsim 50$ nm.

Scattering/Extinction Measurements

If the particles have a refractive index with an imaginary part (i.e., complex refractive index), a combination of calibrated scattering plus extinction measurements can yield the volume equivalent sphere size and number density (Sorensen 2001; Guinier et al. 1955; Sorensen and Shi 2000; Oh and Sorensen 1999; D'Alessio 1981). From Equations (3) and (7), the scattered light intensity is

$$I_s = c P_o n k^4 a^6 F. \quad (18)$$

In Equation (18), c is a calibration constant involving the solid angle of detection, scattering volume length, detector sensitivity, etc., which can be determined by scattering from gases and liquids of known Rayleigh ratio. Recall Equation (9). Table 1 gives some Rayleigh ratios that are useful for calibration.

Extinction is the attenuation of light as it passes through a medium. If I_o is the incident intensity and I is the intensity transmitted after it passes through a length x of the medium, then

$$I = I_o e^{-\tau x}, \quad (19)$$

where τ is the extinction coefficient or turbidity with units of inverse length. Extinction can occur if the light is scattered out of the beam and/or absorbed and changed to another form of energy. Thus, one can show

$$\tau = n(C_{sca} + C_{abs}). \quad (20)$$

In Equation (20), C_{sca} is the total scattering cross section obtained by integrating the differential cross section over all solid angles while accounting for incident polarization perpendicular to the scattering plane. In the Rayleigh regime where there is no angular dependence in the cross section, this integration yields a factor of $8\pi/3$ (Sorensen 2009); thus

$$C_{sca} = \frac{8\pi}{3} k^4 a^6 F \quad (21)$$

for Rayleigh scattering.

The Rayleigh absorption cross section is (Sorensen 2009)

$$C_{abs} = 4\pi k a^3 E \quad (22)$$

where

$$E = \text{Imag} \left[\frac{m^2 - 1}{m^2 + 2} \right]. \quad (23)$$

In the small a limit $C_{abs} \gg C_{sca}$. To see this calculate the ratio from Equations (21) and (22) as

$$\frac{C_{sca}}{C_{abs}} = \frac{2}{3} (ka)^3 F/E. \quad (24)$$

Obviously, as $ka \rightarrow 0$, the ratio approaches zero. It would be computationally convenient to drop C_{sca} from the extinction in Equation (20), but this approximation begins to fail for $a \gtrsim 50$ nm, depending on F/E (for soot $F/E = 0.8$ to 1.6) (Sorensen 2001).

Proceeding without the approximation, Equations (18) and (20) with (21) and (22) can be solved for a and n as

$$a^3 = \frac{4\pi E}{k^3 F} \frac{I_s/cP_o}{\tau - \frac{8\pi}{3} \frac{I_s}{cP_o}} \quad (25)$$

and

$$n = \left(\frac{k}{2\pi} \right)^2 \frac{F}{E^2} \frac{\left(\tau - \frac{8\pi}{3} \frac{I_s}{cP_o} \right)}{I_s/cP_o}. \quad (26)$$

Recall that τ is measured from the extinction measurement and I_s/cP_o is from scattering. In the small particle approximation ($\tau = nC_{abs}$ when $C_{abs} \gg C_{sca}$) the terms involving $8\pi/3$ in Equations (25) and (26) would be eliminated.

How feasible are these measurements? The scattering feasibility was discussed above. To study absorption feasibility we use Equations (20)–(23). Assume $E = 0.2$, a typical value for soot. E values for metal particles typically range from 0.04 to 0.6. Obviously, small E yields weak absorption. A 10% attenuation, i.e., $I/I_o = 0.9$, is easily measured, whereas 1% is difficult. Thus, if the path length is $x = 1$ cm, $\tau = 0.1 \text{ cm}^{-1}$ would be measurable. If $x = 10$ cm, then we require only

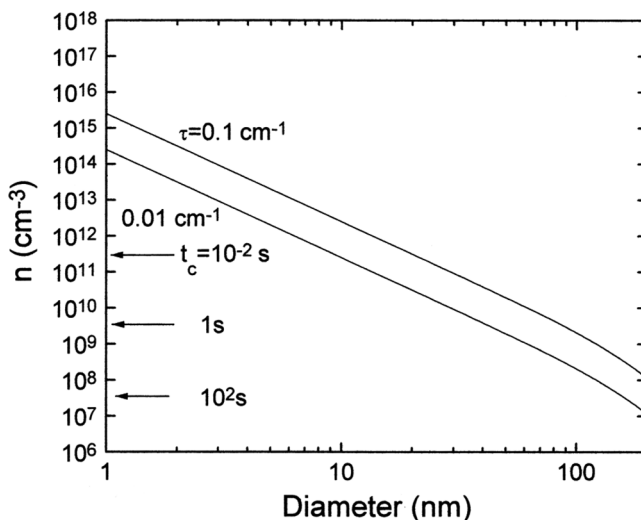


Figure 5. Number density n as a function of particle diameter for different values of the extinction turbidity τ when $\lambda = 500 \text{ nm}$, $m = 1.5$, and $E = 0.2$. Downward curvature when $d \gtrsim 80 \text{ nm}$ is when σ_{sca} in Equation (20) becomes significant. Constant volume fraction lines are parallel to the constant τ lines (for $d < 80 \text{ nm}$); see Figure 2. Also shown are arrows indicating approximate concentrations for three aggregation times t_c for particles in air at $T = 20^\circ\text{C}$ and $p = 1 \text{ atm}$.

$\tau = 0.01 \text{ cm}^{-1}$. Figure 5 shows these two τ -contours on an n versus d graph derived from Equations (20)–(23). As in Figure 2, we also include aggregation time estimates.

Conclusions that can be drawn for nanoparticle extinction measurements are similar to the conclusions for scattering. For example, if we attempt to measure the extinction of a $d = 10 \text{ nm}$ soot or metal particle, we need number concentrations on the order of $n \simeq 3 \times 10^{11} \text{ cm}^{-3}$. This corresponds to a volume fraction of 1.6×10^{-7} . It also will aggregate with $t_c \simeq 10^{-2} \text{ s}$, hence flowing or pulsed systems will be needed.

Dynamic Light Scattering

Dynamic light scattering (DLS) uses the fluctuations in the scattered light intensity to determine particle size (Berne and Pecora 1976). The more rapidly the light fluctuates, the faster the particles are moving, hence the smaller they are. To measure the time scale of the fluctuations a device known as a correlator calculates the intensity correlation function of the scattered light, which has the general form

$$\langle I(0)I(t) \rangle \equiv C(t) = B + Ae^{-t/\tau_c}. \quad (27)$$

In Equation (27) A and B are constants, and $\langle \dots \rangle$ means a time average. Size information resides in the correlation time, which, under the assumption of homodyne detection (Berne and Pecora 1976), is

$$\tau_c = (2Dq^2)^{-1} \quad (28)$$

where D is the diffusion coefficient of the particles.

Nanoparticles are very likely not in the continuum regime where the Knudsen number,

$$Kn = mfp/a \quad (29)$$

is essentially zero. In Equation (29) mfp is the mean free path of the medium molecules. To describe D for all Kn , one usually uses the transcendental Cunningham correction to the Stokes-Einstein form of D (Seinfeld 1986). We have shown that a much simpler equation is nearly as accurate and much easier to use (Sorensen and Wang 2000); it is

$$D = \frac{k_B T}{6\pi\eta a} (1 + 1.612 Kn). \quad (30)$$

In Equation (30) the first term is the Stokes-Einstein form for the diffusion coefficient, with k_B representing Boltzmann's constant, T the temperature, and η the shear viscosity. With this, the basic idea of DLS is to measure τ_c , determine D , and then invert (30) (with (29)) to determine the radius, a .

Effective DLS measurements of particle size in the nano-regime will require both enough scattered light and τ_c in a range in which it can be measured. The scattered light was discussed above. For DLS to be efficient, however, the scattered light must be more than visible; there must be at least a small probability of a photocount emitted from the detector in a time interval equal to τ_c . Thus, when τ_c is small, which it is for small particles, more scattered light intensity is needed. Since this is a function of τ_c , we first determine the τ_c range possible, then return to the problem of scattered intensity.

Correlation Times for DLS

We will calculate correlation times for light scattered from particles in air at atmospheric pressure. Results will be similar for other light gasses. Both $T = 20^\circ\text{C}$ and 2000°C will be considered. The viscosity of air is $\eta = 180 \mu\text{P}$ and $651 \mu\text{P}$ at these temperatures, respectively (*Handbook of Chemistry and Physics* 1976). The gas molecule mean free path can be determined from (Sorensen and Wang 2000)

$$mfp = \eta/0.491\rho\bar{c} \quad (31)$$

where ρ is the mass density, the average speed is

$$\bar{c} = (8k_B T/\pi m)^{1/2} \quad (32)$$

and m is the molecular mass. These equations yield $mfp = 66 \text{ nm}$ at 20°C and 666 nm at 2000°C .

For q again use $\lambda = 500 \text{ nm}$. The scattering angle θ will be a parameter held constant as τ_c versus diameter is explored. Equations (14) and (28–30) are now used to calculate τ_c .

Figures 6 and 7 show results for $T = 20^\circ\text{C}$ and 2000°C , respectively. Although most commercial correlators have a fastest time scale of $0.2 \mu\text{s}$, time scales less than $\sim 3 \mu\text{s}$ are usually perturbed by photomultiplier after-pulsing. So we will use $\tau_c \gtrsim 3 \mu\text{s}$

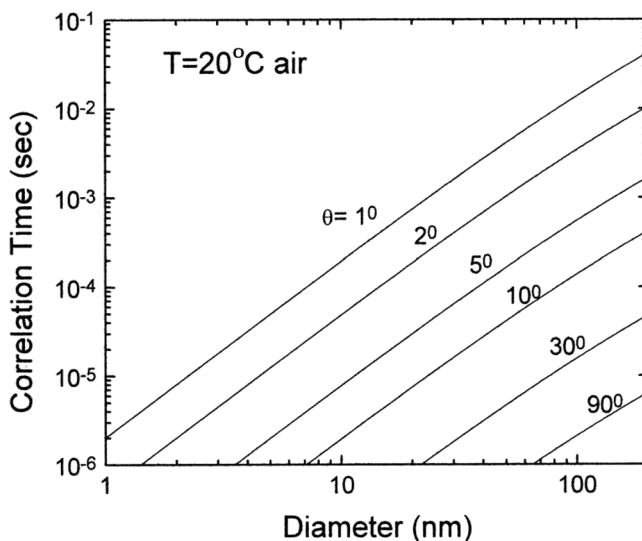


Figure 6. DLS correlation time vs. diameter for particles in air at $T = 20^\circ\text{C}$ and $p = 1$ atm for different scattering angles, θ , at $\lambda = 500$ nm.

as the experimentally viable range. Because the particles are so small, Equations (28) and (30) tell us that q , hence θ , must be small to keep $\tau_c \gtrsim 3 \mu\text{s}$. Small scattering angles present a number of experimental problems. If the aerosol is in any manner contained, then the laser beam must enter and exit the aerosol chamber through windows. All windows scatter significantly in the forward direction, especially $\theta \lesssim 5^\circ$. This is due to imperfections on the window surface and dirt on the surface. Dirt can, with care, be removed, but rare is the environment where it does not reappear with

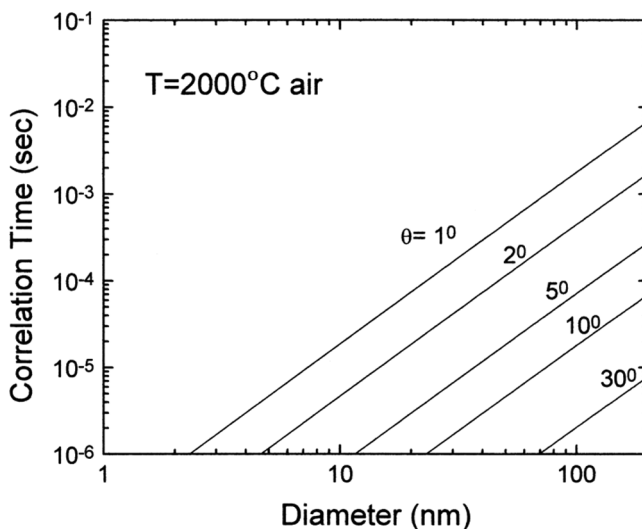


Figure 7. DLS correlation time vs. diameter for particles in air at $T = 2000^\circ\text{C}$ and $p = 1$ atm for different scattering angles, θ , at $\lambda = 500$ nm.

time. Moreover, cleaning can scratch the surface, and scratches are a source of forward scattering. Surface imperfections can be improved with high-quality optical windows of low “scratch and dig” and coated. Regardless, $\theta < 5^\circ$ is difficult.

Incident beam convergence and collection solid angle imply some $\delta\theta \neq 0$ to limit θ because to precisely define q we require $\theta \gg \delta\theta$. Typically, this is on the order of $\delta\theta \simeq 0.5^\circ$. For example, a 20 cm focal length lens focusing a 0.1 cm waist laser beam has $\delta\theta \simeq 0.3^\circ$. Small θ implies the photosensitive area must be far away so not to intersect the incident beam. Consequently, this decreases the scattered power.

In summary, we will use $\theta = 5^\circ$ as a lower limit that is experimentally accessible. Then, if we require $\tau_c \geq 3 \mu\text{s}$, we see from Figures 6 and 7 that DLS is limited to $d \gtrsim 7 \text{ nm}$ at $T = 20^\circ\text{C}$ and $d \gtrsim 20 \text{ nm}$ at $T = 2000^\circ\text{C}$.

Scattered Intensity for DLS

An important factor involved in DLS is to have a photocount rate large enough so that the photocounts per correlation time are on the order of 0.1 or more. This value is an order of magnitude prescription based largely on this author’s experience. Photocount rates of 0.01 per τ_c result in very slow accumulation of the correlation function by the correlator. Figures 6 and 7 show that τ_c will be on the order of 10^{-5} s for nanoparticles, thus we require photocount rates of about $0.1 \text{ count}/10^{-5} \text{ sec} = 10^4 \text{ counts/s}$. As an example, recall the discussion above for absolute scattering strength and realize that that magnitude of the photocount rate from a PMT with 10% quantum efficiency would require incident powers of 0.1 watt if $R_{vu} \simeq 10^{-8} \text{ cm}^{-1} \text{ sr}^{-1}$. With DLS, the scattering from the medium gas, most typically air, is much less important than for SLS because the medium’s dynamic information is at much shorter time scales than that from the particles. Thus, the correlation function of the possibly weaker particle scattered light can still be measured. Given $R_{vu} \simeq 10^{-8} \text{ cm}^{-1} \text{ sr}^{-1}$, Figure 2 can be used to determine various combinations of n and d that are feasible.

DLS of Flowing Aerosols

We have discussed how the large number densities necessary to create observable scattered light from nanoparticle aerosols lead to rapid aggregation and hence the possible need to use flowing systems. With DLS, however, one must beware because flow can introduce new time scales into the correlation function that can have an effect on particle sizing.

The intensity correlation function for a flowing aerosol is described by (Chowdhury et al. 1984; Taylor and Sorensen 1986)

$$C(t) = B + A_1 e^{-t/\tau_c - t^2/\tau_2^2} + A_2 e^{-t^2/\tau_3^2}. \quad (33)$$

In Equation (33) B is a background, the second term is called the coherent term, and the third the incoherent term. Also in Equation (33)

$$\tau_2 = w_o/v \quad (34)$$

and

$$\tau_3 = w/v. \quad (35)$$

where v is the velocity of the flowing aerosol assumed to be perpendicular to the scattering plane, w_o is the incident beam waist at the focus of the lens that directs the beam toward the scattering volume, and $w \geq w_o$ is the waist at the scattering volume.

Problems can arise in measuring τ_c when the coherent beam transit term interferes. This happens when $\tau_2 \lesssim 10\tau_c$. To estimate τ_2 let $w_o \simeq 75 \mu\text{m}$. This is typical of a 30 cm focal length lens converging the beam of an Argon ion laser. Next assume $v = 1 \text{ m/s}$. This would be a fast flame. Then by Equation (34), $\tau_2 = 75 \mu\text{s}$. This is much larger than the expected τ_c values for nanoparticles that are on the order of $10 \mu\text{s}$ or less (Figures 6 and 7). So there appears to be no problem here. However, some of the high number densities necessary imply short aggregation times t_c , which may require very fast flows. If so, the experimentalist must be aware of this effect.

Conclusions

Light scattering as a probe of nanoparticle aerosols presents many difficulties, most of which are due to the approximately two orders of magnitude difference between the particle size and the optical wavelength. The magnitude of the scattering or extinction will be very weak and comparable to the background gas unless particle number densities are large. Large number densities imply that the aerosol will not be a nanoparticle system soon, because rapid aggregation will ensue. Thus, flowing or pulsed techniques will be necessary to freeze time. Even with adequate light scattering, size determination by scattering anisotropy is limited to perhaps $d \gtrsim 50 \text{ nm}$ unless very precise methods of anisotropy measurement are developed. Combined scattering and extinction may well measure into the nanometer regime but such measurements are limited to particles with complex refractive indices. Dynamic light scattering will require very small scattering angles to produce measurable correlation times for nanoparticles. There is no inherent reason why this cannot be done. Any pulsed technique applied to DLS must have the pulse orders of magnitude longer than the correlation time, thus flowing methods seem best suited for DLS to avoid changes in the aerosol due to aggregation.

Application of light scattering to nanoparticle aerosols is daunting, but we should not decline the challenge. Light scattering, and wave scattering (X-rays, neutrons, electrons, etc.) in general, has been a major factor in uncovering the nature of condensed matter systems throughout the twentieth century. With this heritage, it is reasonable to forecast that light scattering applied to nanoparticle aerosols will be very useful, once the technical problems are overcome. It is up to us to be clever and solve these problems. The present article has displayed conditions under which this endeavor must proceed.

References

- Berne, B. J., and P. Pecora. 1976. *Dynamic Light Scattering*. New York: John Wiley.
- Chowdhury, D., C. M. Sorensen, T. Taylor, J. F. Merklin, and T. W. Lester. 1984. Application of photon correlation spectroscopy to flowing Brownian motion systems. *Appl. Opt.* 23: 4149–4154.
- D'Alessio, A. 1981. Laser light scattering and fluorescence diagnostics of rich flames. In *Particulate Carbon*, ed. by D. C. Siegla and G. W. Smith. New York: Plenum. pp. 207–259.

- Gangopadhyay, C., I. Elminyaw, and C. M. Sorensen. 1991. Optical structure factor measurements of soot particles in a premixed flame. *Appl. Opt.* 30: 4859–4864.
- Guinier, A., G. Fournet, C. B. Walker, and K. L. Yudowitch. 1955. *Small Angle Scattering of X-Rays*. New York: John Wiley.
- Handbook of Chemistry and Physics*, 57th ed. 1976. CRC Press.
- Kerker, M. 1969. *The Scattering of Light and Other Electromagnetic Radiation*. New York: Academic.
- Kim, W. G., C. M. Sorensen, D. Fry, and A. Chakrabarti. 2006. Soot aggregates, superaggregates and gel-like networks in laminar diffusion flames. *J. Aerosol Sci.* 37: 386–401.
- Oh, C., and C. M. Sorensen. 1997. Light scattering study of fractal cluster aggregation near the free molecular regime. *J. Aerosol Sci.* 28: 937–957.
- Oh, C., and C. M. Sorensen. 1999. Scaling approach for the structure factor of a generalized system of scatterers. *J. Nanopart. Res.* 1: 369–377.
- Seinfeld, J. H. 1986. *Atmospheric Chemistry and Physics of Air Pollution*. New York: John Wiley.
- Sorensen, C. M. 2001. Light scattering from fractal aggregates. A review. *Aerosol Sci. Technol.* 35: 648–687.
- Sorensen, C. M. 2009. Scattering and absorption of light by particles and aggregates. In *Handbook of Surface and Colloid Chemistry*, 3rd ed., ed. by K. S. Birdi. Boca Raton, Fla.: CRC Press. pp. 719–745.
- Sorensen, C. M., and D. Shi. 2000. Guinier analysis for homogeneous dielectric spheres of arbitrary size. *Opt. Commun.* 178: 31–36.
- Sorensen, C. M., and G. M. Wang. 2000. Note on the correction for diffusion and drag in the slip regime. *Aerosol Sci. Technol.* 33: 353–356.
- Sorensen, C. M., J. Cai, and N. Lu. 1992. Light scattering measurements of monomer size, monomers per aggregate, and fractal dimension for soot aggregates in flames. *Appl. Opt.* 31: 6547–6557.
- Taylor, T. W., and C. M. Sorensen. (1986). Gaussian beam effects on the photon correlation spectrum from a flowing Brownian motion system. *Appl. Opt.* 25: 2421–2426.